Influence of Thermal Cutting and Its Quality on the Fatigue Strength of Steel

Levels of cutting quality are classified by surface roughness measurements which are then shown to be directly related to fatigue strength

BY F. GOLDBERG

ABSTRACT. Structurals are often fabricated by assembling and welding components that have been thermally cut from steel plate. It is therefore important to know how the quality of the thermal cutting* affects the fatigue strength of dynamically loaded structural members.

This investigation tested plate specimens grouped in five series according to quality of cut, as follows: machined, high quality oxygen cut, normal quality oxygen cut, low quality oxygen cut and normal quality plasma-arc cut. A few specimens with defects were also tested.

To measure the quality of the thermal cutting a special electronic profile measuring instrument was developed. The fatigue testing results were plotted in Wöhler (S-N) diagrams which show that there is nearly a linear relation between surface roughness and fatigue strength. The plasma cut specimens had a fatigue strength comparable with machined specimens. Defects in the thermal cut surfaces had a strong negative influence on fatigue strength. High quality thermal cut specimens had a fatigue strength that was 80% of the yield stress, while low quality specimens had a fatigue strength 60% of the yield stress.

Microstructural examination showed that the serrations caused by the oxygen cutting jet consists mainly of carburized material.

Microhardness measurements showed that there is a soft zone just behind the hard carburized material on the cut surface. This 50μm wide zone has not been observed before.

Introduction

Steel structures often make use of beams fabricated by thermal cutting of steel plates and welding of the flanges to the web, instead of hot rolled mill shapes. The fabrication of beams by thermal cutting and welding gives the designer of steel structures more flexibility since he is not limited to the standard shapes rolled by the mill.

Thermal cut plate edges may exhibit a more or less rough surface caused by the action of the cutting jet and by the vibration of the cutting machine. It is often stipulated in structural codes that all cut surfaces not subjected to welding are to be ground free of serrations, especially if the surfaces are on a part that is dynamically loaded. Because grinding or milling of such surfaces is very costly, it is important to know how the thermal cut surface and its quality affects the steel.

FRED GOLDBERG is Assistant Professor, Department of Welding Technology, The Royal Institute of Technology, Stockholm, Sweden.

Paper is under consideration by Commission 1 of the International Institute of Welding (IIW document I-483-72).

**The term thermal cutting is used throughout this paper where reference to both oxygen cutting and plasma-arc cutting is intended.*

The aim of this investigation has therefore been to study the relationship between the quality of the thermal cut surface and fatigue strength. Similar investigations involving oxygen cutting have been made before, but in none of them have the quality of the cuts been recorded with accuracy. The test specimens have also been small. This investigation did not encompass a study of cut surfaces that were subsequently welded to other components of a structure.

The testing was done at the Department of Welding Technology at the Royal Institute of Technology, Stockholm, using a 150 ton fatigue testing machine, which is one of the heaviest in Sweden. This machine made it possible to test pieces that have the same thickness as flanges in large steel structures. The investigation was partly financed by a grant from the Swedish Board of Technical Development.

Experimental Details

Material

Steel St 52-3, which corresponds to ASTM A572, Grade 55, was selected for this investigation. This steel was 30mm (1.2 in.) thick, micro-alloyed with columbium and normalized. The analysis is given in Table 1.

Table 1 — Composition (Wt%) and Properties of Steel St 52-3 [a]

C	Si	Mn	P	S	Cr	Ni	N	Al	Cb
0.18	0.47	1.40	0.020	0.022	0.01	0.02	0.005	0.008	0.025

Tensile strength, kg/mm² (ksi)	59.9	(85.2)
Yield strength, kg/mm²(ksi)	40.5	(57.5)
Elongation in 50 mm (2 in.), %	26.4	
Charpy-V impact strength at 0C (32F), kgm (ft-lb)	7.3	(52.8)

(a) Equivalent to ASTM A572, Grade 55.

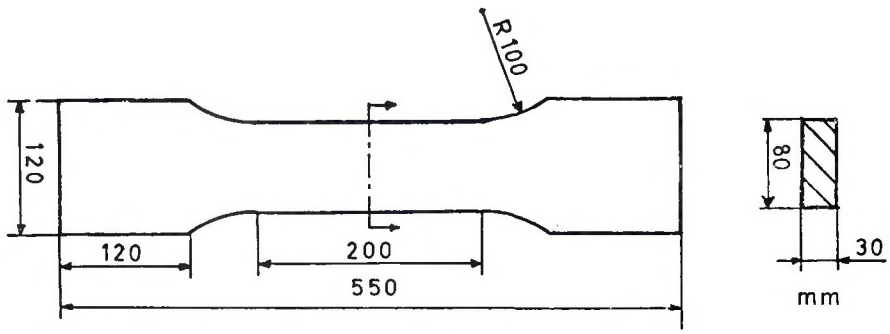

Fig. 1 — Test specimen, dimensions in millimeters (1 in. = 25.4 mm)

Test Specimens

To make this investigation as realistic as possible, it was decided to use a plate thickness of 30 mm (1.2 in.) which might be used in larger steel structures. The design of the test specimen (Fig. 1) was then limited only by the capacity of the fatigue testing machine.

The following series of test specimens was prepared, the number of specimens for each series ranging from four to twelve:

A. Machined edge
B. Oxygen cut edge, high quality
C. Oxygen cut edge, normal quality
D. Oxygen cut edge, poor quality
E. Plasma-arc cut edge, normal quality

All material for this investigation came from the same heat. All test specimens were cut from the same steel plate in a small machine cutting unit using a magnetic roller on a steel template. After cutting, all specimens had their radii machined free from serrations. Mill scale was not removed, but all corners were chamfered about 2 mm (0.08 in.), Fig. 2.

When fabricating series A, the specimens were first oxygen cut using the template with a correction for the width of the specimens. Then the specimens were machined to the correct size. The machined surface was of high quality.

Series B was made by using a special acetylene tip designed by the author to give high quality cuts. The cutting speed was 450 mm/min (17.7 ipm).

For series C and D an ordinary acetylene tip with a divergent cutting orifice was used. The cutting speed varied between 300-400 mm/min (11.8-15.7 ipm). To obtain the rough surfaces of series D, the cutting torch was put into vibration by manually shaking the traverse beam on the cutting machine. In workshops, rough cut surfaces are caused mostly by vibrations from an overhead crane, a heavy truck passing by, dropping of heavy objects, or by unevenness and unclean rails of the cutting machine. Some cutting machines may vibrate when the machine moves or changes direction.

For making the specimens in series E, a 30 kW plasma-arc cutting unit was used. The plasma gas was 80% argon, 20% hydrogen, and the cutting speed 400-500 mm/min (15.7-19.7 ipm). The plasma torch was mounted on the same cutting machine and the same template was used.

When fabricating the specimens, notches were purposely made on some for comparison tests. One specimen was plasma-cut with a damaged nozzle causing a rough surface. These specimens were fatigue tested but were not included in the Wohler curves (S-N curves).

Testing Machine

A MTS fatigue testing machine was used having a maximum capacity of ± 150 tons for fatigue testing. For this study a haversine cycle giving a minimum stress of +3 kg/mm² (4270 psi) per cycle was used. The frequency varied between 5-6 hertz depending on the load.

Instrument for Profile Measurements

A number of investigations concerning the fatigue strength of oxygen cut surfaces has been carried out, but in none of them has the quality of the cut surface been recorded with accuracy. Some have been referred to as being of high quality or of poor quality. These definitions are neither scientific nor satisfactory. In one investigation two companies were asked to cut test specimens of good and poor quality for a fatigue test. It turned out that the poor quality from one factory was about equal to the good quality from the other. An important part of this investigation has been to measure the quality of the thermal cut surface.

When discussing the quality of the cut surface many different factors may be taken into consideration, such as:

1. Depth of the serrations (roughness)
2. Amount of drag depending on the cutting speed
3. Accuracy of the bevel of the cut

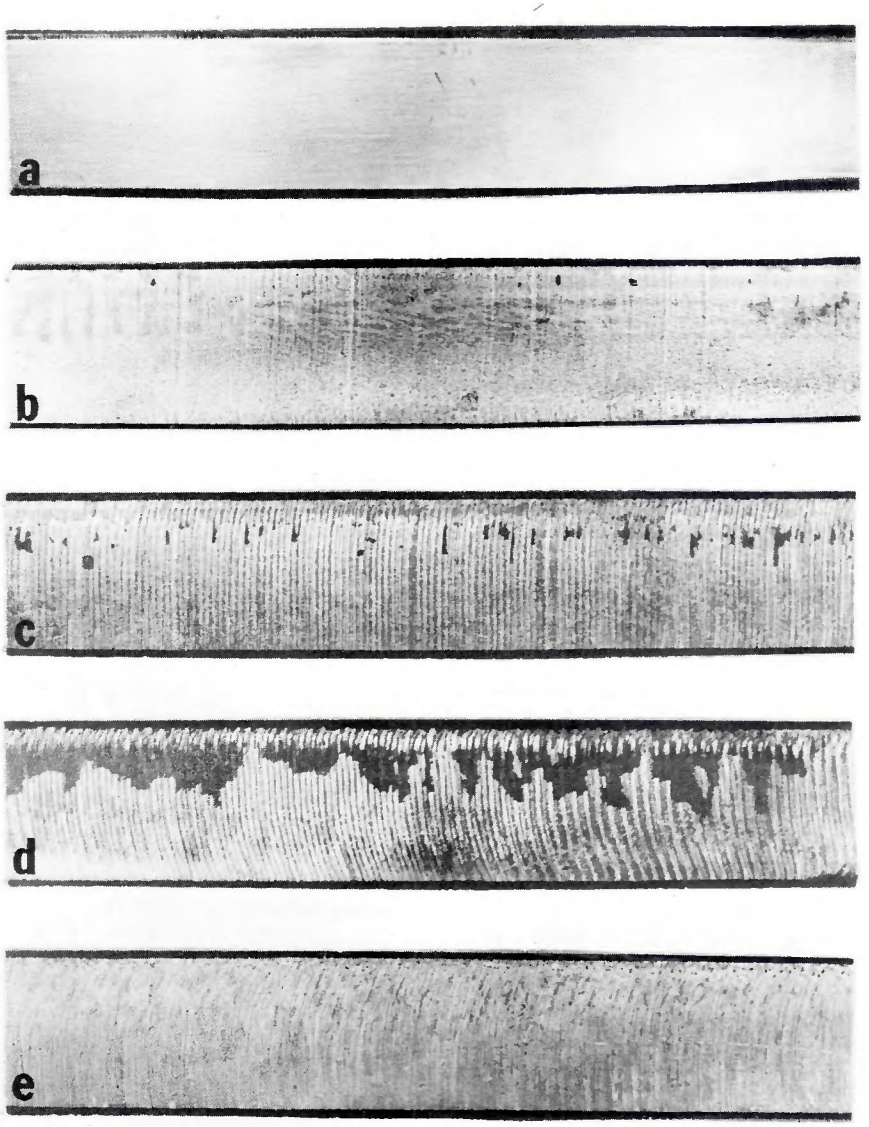

Fig. 2 — Thermal cut surfaces of various qualities. (a) high quality machined, (b) high quality oxygen cut, (c) normal quality oxygen cut, (d) low quality oxygen cut, (e) a normal quality plasma arc cut

4. Flatness of the cut surface (convex or concave)
5. Condition of the upper and lower edges
6. Condition of slag and its adhesion

Of the abovementioned factors numbers 1 and 5 are the most important in connection with fatigue (Ref. 4). As all specimens have their upper and lower edges chamfered there is only factor 1 to take into consideration. Surprisingly enough it was found to be very difficult to measure the profile of the thermal cut surface.

A special profile measuring instrument was therefore designed and built by the author. It consists of a needle connected to a differential transformer. When the needle is set to run along the cut surface, by help of a milling machine, Fig. 3, the signals are transformed electronically and presented in a digital form in microns (μm) in relation to a zero-reference plane. The needle has a 30 deg tip with a radius of 0.25 mm (0.01 in.). In parallel a pen recorder is connected to the digital readout and displays the profile on paper.

All the test specimens were measured with this instrument on the same side where the fracture initiated, and on specimens that did not fracture, the roughest side was measured.

Results

Microstructural Examination

In each series of test specimens one specimen was taken out and cut perpendicular to the thermal cut surface. The following descriptions refer to the material in the center of the cut surface when regarded in the thickness direction, perpendicular to the cutting direction. All specimens, with the exception of those machined, have a larger heat-affected zone along the upper side of the specimens due to the heating flames from the cutting nozzle. The temperature gradient here is not as steep as further down the kerf.

Machined Specimen. As expected, this piece showed only the original microstructure of the steel which consist of ferrite and pearlite in a typical band structure.

High Quality Oxygen Cut Specimen. Starting at the cut surface, the

Fig. 3 — The profile measuring instrument mounted on a milling machine

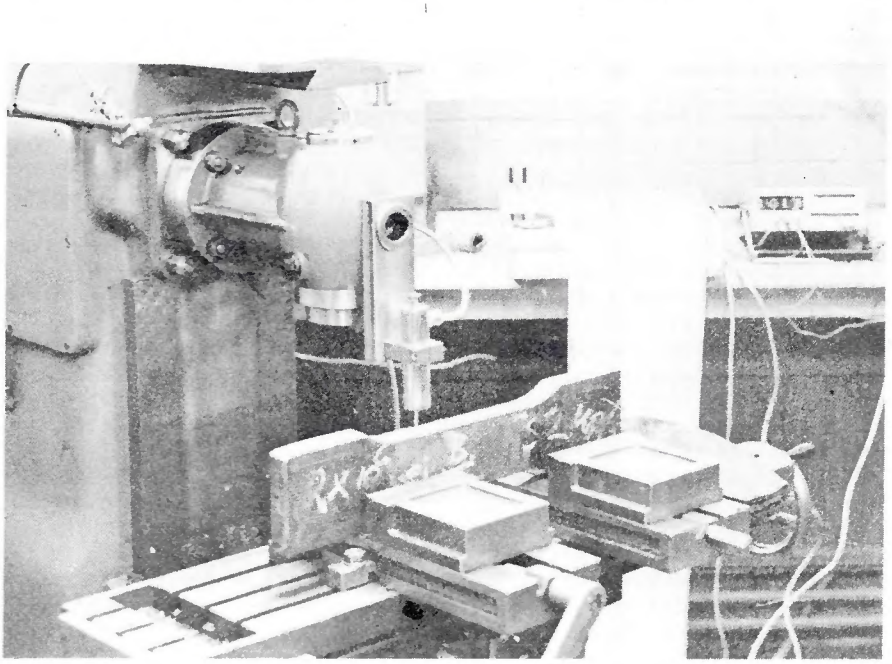

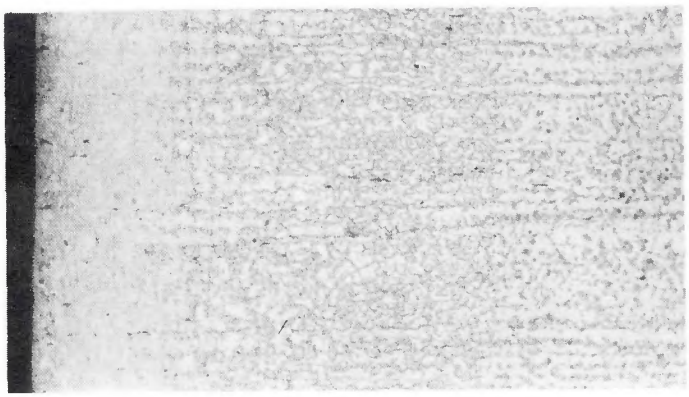

Fig. 4 — The microstructure adjacent to the oxygen cut surface, X100, reduced 23%

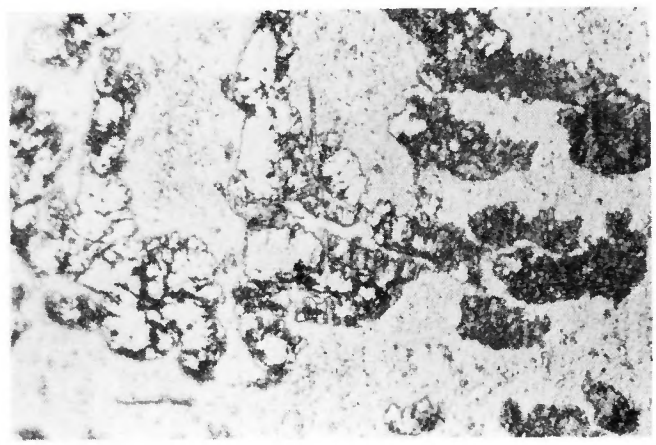

Fig. 5 — The border-line between the partially transformed zone and the original structure 1.2 mm (0.060 in.) from the oxygen cut surface. X400, reduced 23%

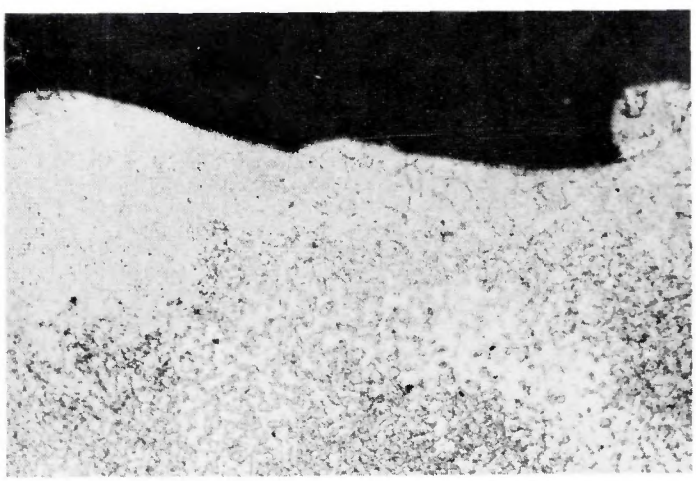

Fig. 6 — Micrograph taken in the center of the plate perpendicular to the cut surface showing 3 serrations. The serration in the center consists mainly of carburized material while the two other serrations mainly are carburized on the left side. The direction of the cutting jet was from right to left which means that the carburized material is found "behind" the larger serrations. Specimen C2, 140 μm (0.0056 in.) surface roughness

microstructure consists of a very thin layer that has been carburized due to selective oxidation by the oxygen cutting jet (Refs. 1, 2). The carburized layer consists of spots of ledeburite on top of a 50 μm (0.002 in.) thick high carbon structure-free martensite containing spots of troostite and bainite, Fig. 4. Behind the carburized layer the structure is a matrix of martensite, tempered martensite and bainite. As this matrix contains no carburized material its carbon content is the same as that in the original material. About 0.5 mm (0.02 in.) from the cut surface the matrix is formed into a structure consisting of martensite grains, some pearlite and ferrite — in welding technology known as "partially transformed zone". At 1.2 mm (0.060 in.) from the cut surface, the martensite grains in the pearlite disappear and the original structure is found.

This heat-affected zone, 1.2 mm in width, indicates that the temperature within this zone has exceeded 728 C (1350 F) or the A_1-level in the Fe-C phase diagram. The pearlite that exceeds this temperature transforms into austenite and, at the following quick cooling, martensite is formed, giving a band structure of martensite grains and ferrite (Ref. 3). The borderline for this transformation is mostly very sharp due to the steep temperature gradient during cutting, Fig. 5 (Ref. 5).

Normal Quality Oxygen Cut Surface. The microstructure of the oxygen cut specimens of normal quality is very similar to the one described above. The total heat-affected zone is 0.9 mm (0.036 in.), the martensite matrix 0.4 mm (0.016 in.) and the carburized layer varying in thickness between 10-60 μm (0.0004-0.0024 in.). It is interesting to note that the thickness of the carburized layer is larger on top of a serration than between two serrations, Fig. 6. Smaller serrations consist entirely of carburized material.

Low Quality Oxygen Cut Specimens. The microstructure of these specimens was identical with the normal quality ones.

Plasma-Arc Cut Specimens. The microstructure of plasma-arc cut

specimens is very different from oxygen cut specimens. First, there is no hard carburized layer on the cut surface because there is no oxygen jet present causing a selective oxidation. During plasma-arc cutting, the hot plasma jet melts the material and the kinetic energy of the jet removes the melt thus producing the desired kerf. This process causes a larger heat input in the material which results in a larger heat-affected zone (Ref. 6).

Instead of a carburized layer there is a layer, approximately of the same thickness as the carburized layer, that has been in a molten state and could be regarded as a cast structure, Fig. 7. The material behind the cast structure is a matrix of martensite, tempered martensite, pearlite, bainite and high carbon retained austenite. This matrix has larger grains than the oxygen cut specimen and it extends 1.5 mm (0.060 in.) from the cut surface, which verifies the larger heat input. Behind the matrix there is a band structure of martensite grains and pearlite, as found in oxygen cut specimens, but this partially transformed zone is not so distinct because of the larger heat input making the temperature gradient less steep. The total heat-affected zone was about 3 mm (0.120 in.)

Fig. 7 — The microstructure adjacent to the plasma-arc cut surface

Microhardness

A series of hardness measurements was made with a Reichert microhardness measuring instrument using a load of 50 g. The measurement from one specimen of each series was made in the center of the cut surface going from the outer carburized layer into the material, Fig. 8. The results are displayed in Fig. 9.

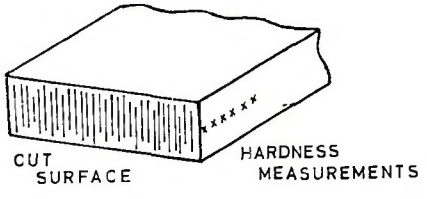

Fig. 8 — Method of microhardness survey

When displaying microhardness, one must take into consideration that each measurement is usually made on a single grain, and the hardness obtained depends on the type of microstructure measured. Therefore it is logical to display on the diagrams approximate areas that include the different hardnesses found at the same distance from the cutting surface. When looking at the hardness diagrams of the oxygen cut surfaces it is interesting to note that just behind the fusion zone between the carburized layer and the matrix of martensite the hardness curve has a minimum point. The hardness has here suddenly dropped to 450-500 MHV before it increases to 600-700 MHV further into the martensite matrix. This softer zone is only about 50 μm (0.002 in.) wide which might explain why this drop in hardness has not been observed before. The microstructure of this zone is very similar to the martensite matrix but had a darker shade when etched in 1 % nital, Fig. 10.

Another possibility is that this dark structure is a low temperature bainite. About 0.5 mm (0.02 in.) from the cut surface the martensite matrix transforms slowly into a band structure of martensite grains and ferrite. In the hardness diagram this area shows a maximum around 700-800 MHV which is the hardness of the martensite grains. The lower value gives the hardness in the ferrite band. Further to the right the hardness area converges where the upper line limits the hardness in the pearlite and the lower indicates the hardness in pure ferrite.

Results of Profile Measurements

The results of the profile measurements are listed in Table 2. Each specimen was measured on the roughest area of the cut surface and the highest figure found on the diagram is listed in the table. Figure 11 shows a typical profile from each series. It should be noted that the true profile has been enlarged 200 times in the depth direction and only 16 times in the width.

The profiles from normal to bad quality oxygen cut specimens show a regular wave form due to the serrations. It is therefore interesting to note that the high quality oxygen cut specimens and the plasma arc cut specimens have a very irregular profile with small amplitude variations.

Fatigue Test Results

All fatigue tested specimens are listed with their respective data in Table 2. After the specimens had their profile measured they were divided into three quality groups.

Quality	Max. profile depth, μm
High	<100
Normal	100-200
Low	>200

A Wöhler curve was plotted for each of the three quality groups and for the machined and plasma-cut specimens. Each curve is plotted in a double-logarithmic diagram. The data points are marked with a + and connected with a curve of the type log $S = A_2 \log^2 N + A_1 \log N + A_0$ calculated with the method of least squares, Fig. 12. The scatter is calculated with the formula.

$$s = \left[\sum (S-S_N)^2/(n-3) \right]^{1/2}$$

where
S = y-coordinate of the plotted curve for a certain value of N (cycles)
S_N = y-coordinate for a certain data point
n = number of data points
3 = the number of degrees of freedom

Machined Specimens. Eleven test pieces were fatigue tested. Of these two specimens had fracture initiation

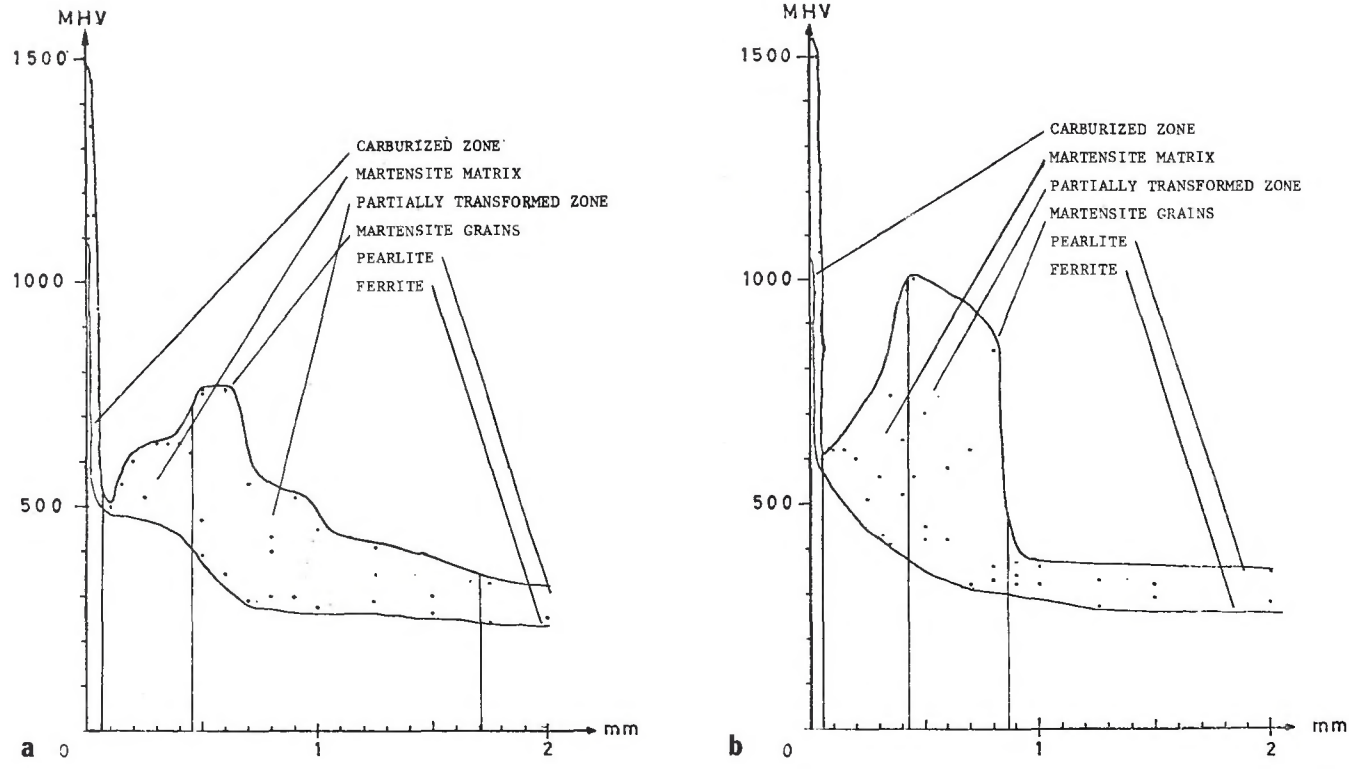

Fig. 9 — Microhardness vs distance from cut surface. (a) high quality oxygen cut surface, (b) normal quality oxygen cut surface, (c) low quality oxygen cut surface, (d) plasma-arc cut surface

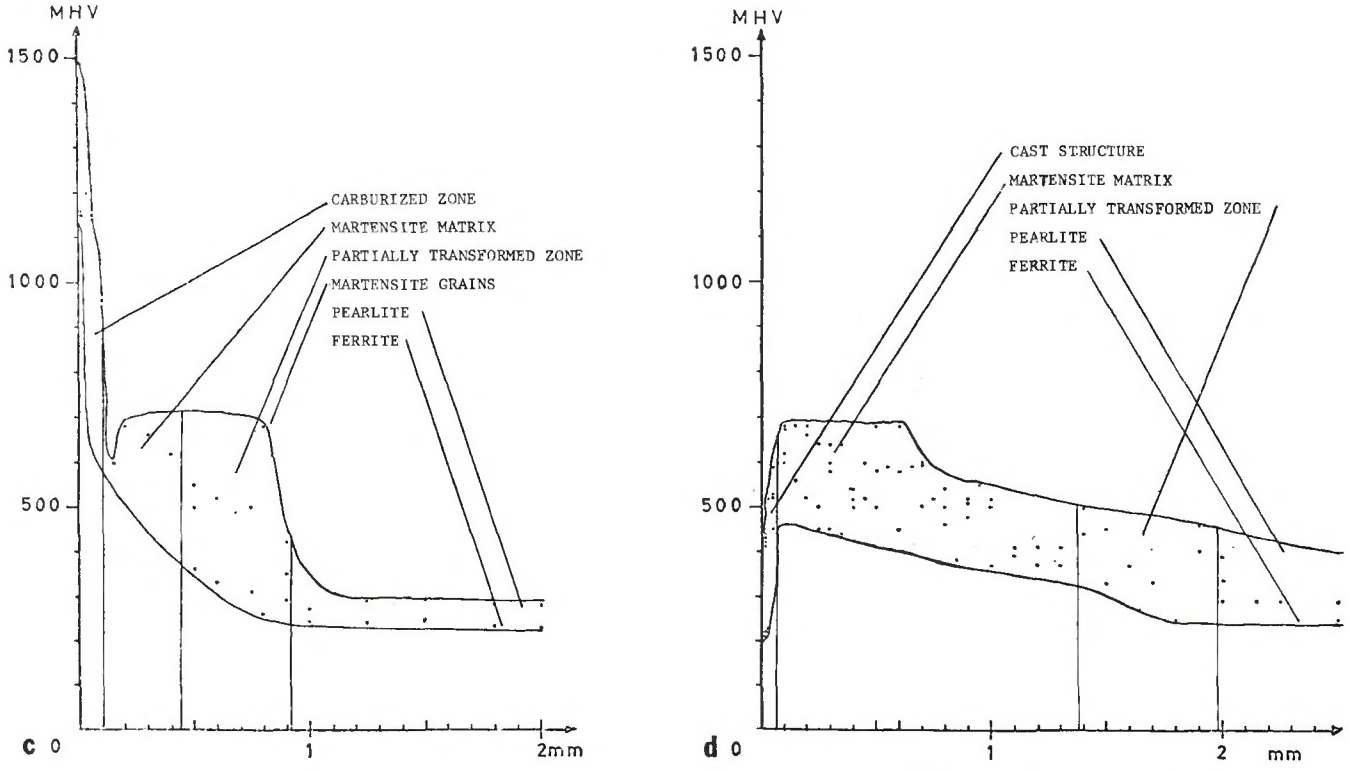

in the mill scale, four on the edge, Fig. 13, one in the machined surface and one in the mill scale due to a defect in the plate. The last one is not included in the Wöhler curve.

From the curve the following data is obtained

σ_{max} = 33 kg/mm² (46.5 ksi) at N = 2 × 10⁶
s = 0.0128 or 3 %

High Quality Specimens. Nine test pieces were fatigue tested. Of these four showed fracture initiations in the lower edge of the kerf and one in the mill scale.

σ_{max} = 32 kg/mm² (45.0 ksi) at N = 2 × 10⁶
s = 0.0087 or 2.0 %

Normal Quality Specimens. Unfortunately only four specimens belonged to the normal quality group of the profile measurements, but the distribution of the four data points made it possible to plot a realistic curve. The fracture initiation point was in one specimen on the cut surface and in two specimens on the upper edge of the kerf.

σ_{max} = 28 kg/mm² (39.5 ksi) at N = 2 × 10⁶
s = 0.0023 or 0.5 %

Low Quality Specimens. The low quality specimens showed the largest scatter in the Wöhler diagram. In this group of specimens, the fracture initiation point is found more frequently at the cut surface than in the other groups. Five specimens had the cut surface as fracture initiation "point," but two of these specimens had defects (notches) in the cut surface and are therefore not included in the Wöhler curve, Fig. 14.

Test pieces D 11 and D 12 had the roughest surfaces (350 μm) but when plotted in the S-N diagram they show much better values than specimens with less rough surfaces. These two specimens are therefore not included in the Wöhler curve representing low quality oxygen cut surfaces. These two specimens will be discussed later.

The fracture initiation point for two specimens was on the upper edge of the kerf and on one specimen, the lower edge of the kerf.

σ_{max} = 25 kg/mm² (33.8 ksi) at N = 2 × 10⁶
s = 0.0338 or 7.8 %

Plasma-cut specimens. Eight plasma-arc cut specimens were fatigue tested, but of these one had a very rough surface because it was fabricated with a defective nozzle, Fig. 15. It is not included in the Wöhler curve but is displayed in the same diagram (Fig. 12e) with a circle. The fracture started in the upper edge of the kerf in three specimens and in the cut surface in the specimen made with the defective nozzle.

σ_{max} = 33 kg/mm² (46.5 ksi) at N = 2 × 10⁶
s = 0.0156 or 3.6 %

Discussion

Rejected Specimens

Fifteen of the test specimens had to

Table 2 — Fatigue Test and Roughness Data for Specimens Grouped According to Cutting Quality

Specimen	Stress, kg/mm²[a]	No. of cycles, Nx10³	Fracture initiation location	Max. profile depth, μm	Profile ratio, D/W[b] x 10⁻²
		Series A, Machined Quality[c]			
A1	38	255	edge	5	0
A2	34	918	mill scale	5	0
A3	38	408	mill scale	5	0
A4	36	861	edge	5	0
A5	36	466	mach. surf.	5	0
A6	35.5	550	edge	5	0
A7	32	2000	———	5	0
A8	34	2000	———	5	0
A9	36	373	edge	5	0
A10	34	2000	———	5	0
A11x	30	322	defect in plate	5	0
		Series B, High Quality Oxygen Cut[d]			
B1	31.5	2195	no facture	40	5.3
B2	32	929	lower edge	20	3.2
B3	34	1026	lower edge	30	6.4
B4	32	2000	———	80	6.0
B5	34	648	lower edge	30	4.0
B6	32	2000	———	25	6.4
B7	36	373	mill scale	30	8.0
B8	34	613	lower edge	50	8.0
B9	32	2000	———	60	8.9
		Series C, Normal Quality Oxygen Cut			
C1	30	434	upper part of cut surface	150	12.3
C2	28	1390	upper edge	140	13.6
C3	28	2000	———	150	14.0
C4	30	402	cut surface	180	12.5
		Series D, Low Quality Oxygen Cut[e]			
D1	34	542	upper edge	230	9.6
D2	32	429	upper edge	200	11.7
D3	28	682	upper surf.	250	15.0
D4	26	687	upper surf.	300	13.5
D5	24	2000	———	250	16.7
D6	26	2000	———	200	17.2
D7	28	629	lower edge	350	14.8
D8	26	996	surface	300	13.7
D9x	24	326	surface	notch	——
D10x	24	725	surface	notch	——
D11x	30	2000	———	350	14.8
D12x	30	2000	———	350	13.7
		Series E, Plasma-arc Normal Quality[f]			
E1	36	477	upper edge	50	5.0
E2	38	396	upper edge	40	4.0
E3	32	2000	———	60	4.8
E4	36	827	surface	40	8.0
E5	32	2145	———	40	6.4
E6	32	2000	———	70	6.0
E7	34	2360	———	80	12.4
E8x	34	197	surface	400	17.2

(a) Multiply kg/mm by 1.419 to get ksi.
(b) D=profile depth; W=width of serrations.
(c) One specimen fractured in the radius; 4 specimens fractured in the gripping area.
(d) Four specimens fractured in the radius; 1 specimen fractured in the gripping area.
(e) Three specimens fractured in the radius.
(f) Two specimens fractured in the radius.

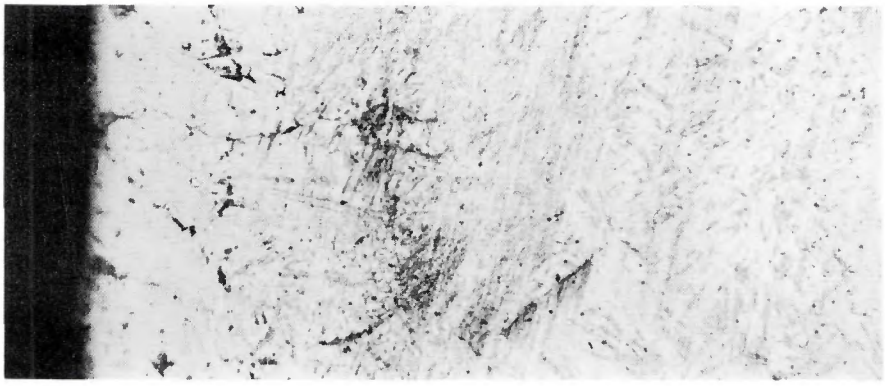

Fig. 10 — The softer material just behind the carburized layer shows a darker structure, probably a low temperature bainite. X500

Fig. 11 — Profile measurements of thermal cut surfaces

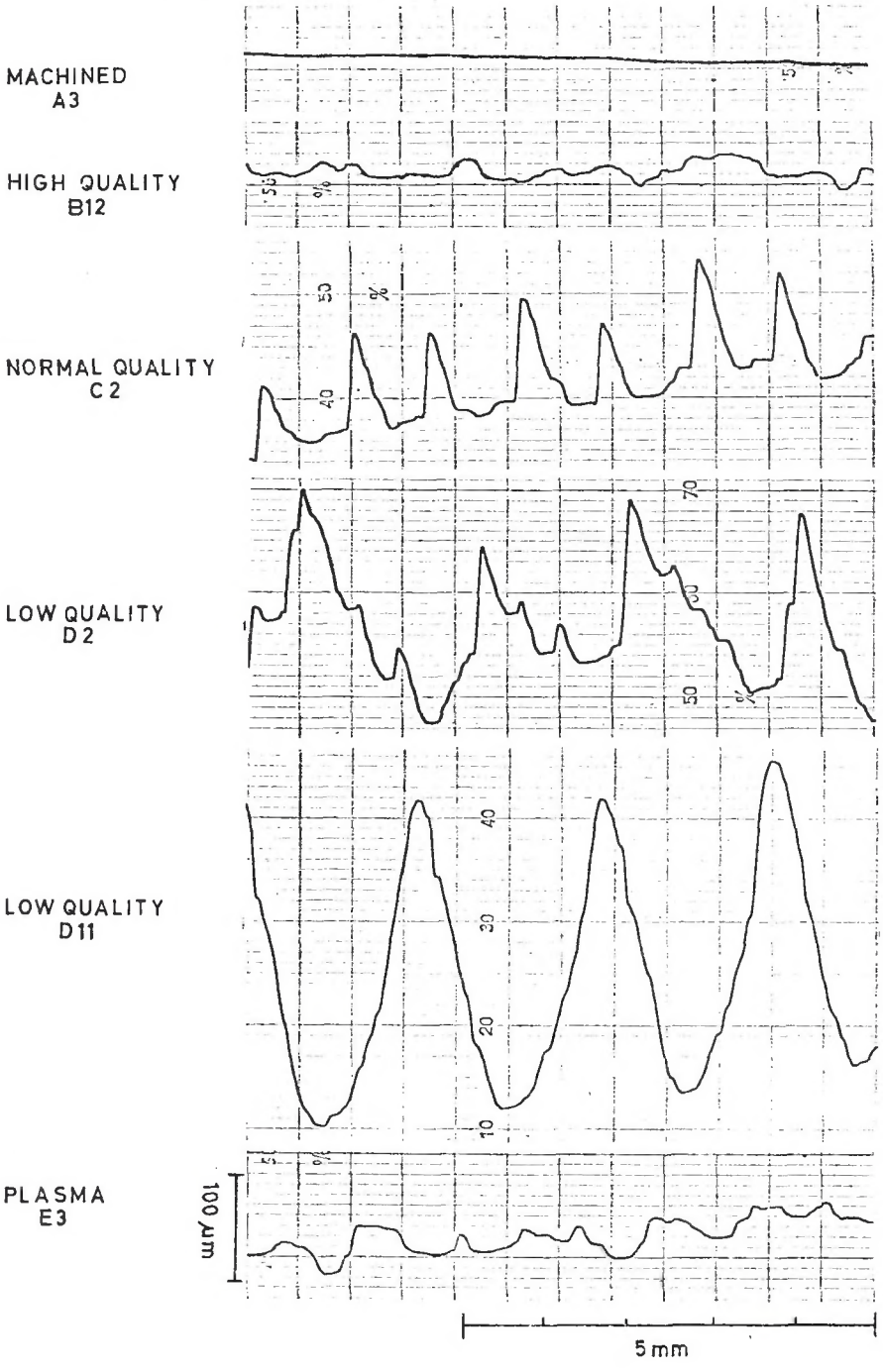

be rejected because of fracture in the radius or in the gripped area of the specimen. Of the total number of specimens the percentage of those rejected is 25%. This must be considered a low value when compared with other investigations where 66% of the specimens were rejected (Refs. 7,8).

At the start of this investigation five specimens fractured in the gripped area. It was then discovered that a number of spikes in the grips were broken, resulting in an uneven distribution of stress to the test piece. When new grips were put into the machine no more fractures of this kind appeared. To avoid fractures in the radius, this portion of the specimen was carefully machined to high quality. The number of the above described fractures in the different series is listed in Table 2.

Quality and Fatigue Strength

When plotting all results from thermal cut surfaces in a S-logN diagram, Fig. 16, they scatter over the whole diagram and give a confusing picture. But if the roughness of each data point is marked a better picture of the situation is achieved. Figure 16 then clearly shows that with decreasing values of roughness the σ_{max} at N = 2 × 10^6 is increasing. If all specimens that ran to 2 × 10^6 cycles are plotted as roughness vs S, as in Fig. 17, it is very interesting to note how the data points lie on a weakly curved line showing the relation between the quality and maximum stress at N = 2 × 10^6 cycles (σ_{max}).

Defects in the Cut Surface

The results from specimens D 9 and D 10 clearly show that defects in the cut surface originating from the cutting operation have a strong influence on the fatigue strength because their notches act as very large stress raisers, Fig. 14. In Fig. 16 these two specimens are plotted with a cross for comparison with the other specimens.

Specimens D 11 and D 12 did not fit into the diagram of Figs. 12 and 17 very well. Even though they have the roughest surface with 350 µm amplitude, they have a much better fatigue resistance than the other specimens in the same series. The explanation is probably to be found in the fact that these specimens have a larger distance between the serrations, Fig. 11, thereby reducing their initiation effect. This is connected with the frequency of the vibrations imposed on the cutting machine. It therefore seems logical to study the initiation effect of a cut surface by dividing the serration amplitude by the width found in the profile measurements.

This ratio is here called "profile ratio" = amplitude/width. The high-

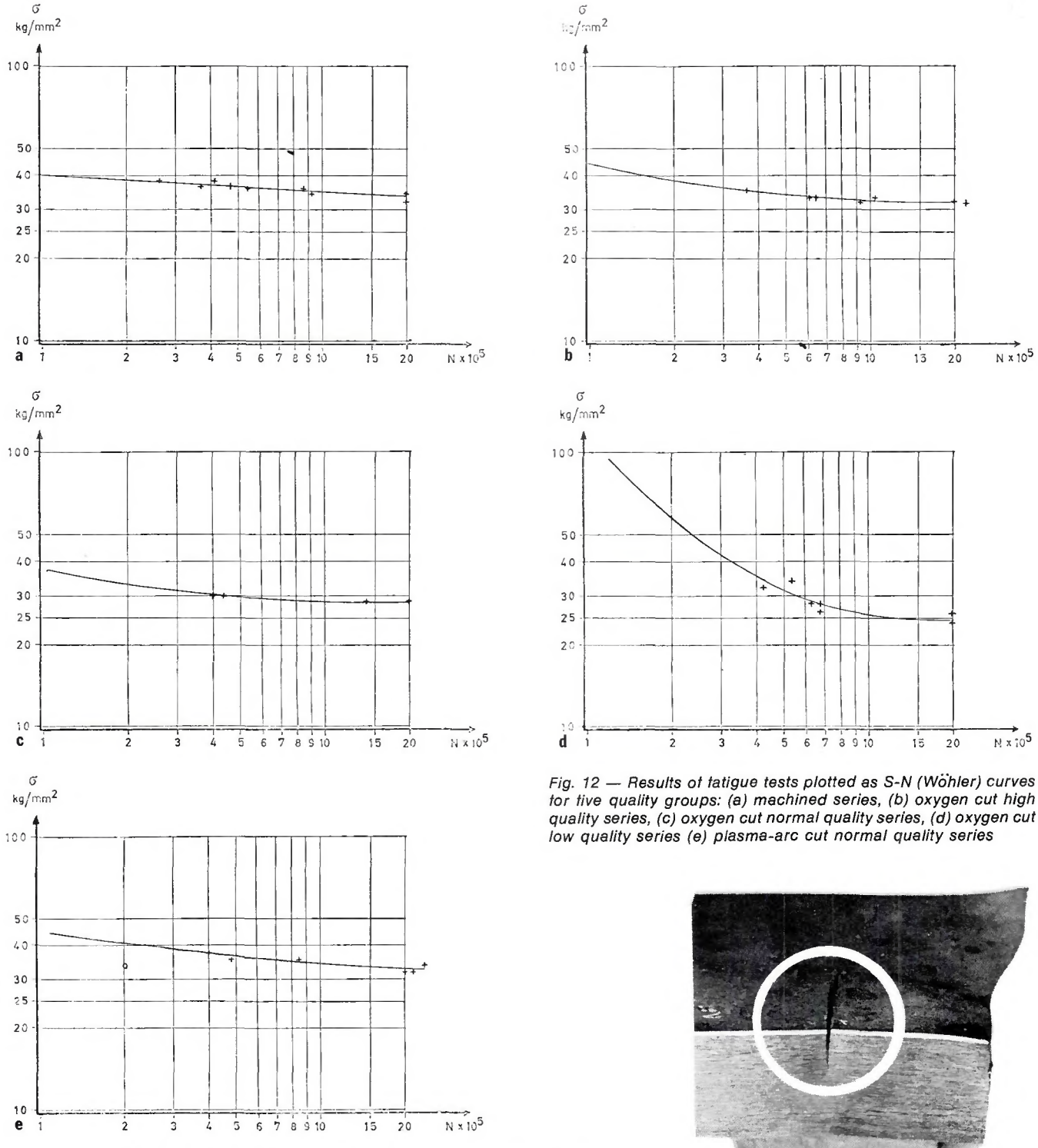

Fig. 12 — Results of fatigue tests plotted as S-N (Wöhler) curves for five quality groups: (a) machined series, (b) oxygen cut high quality series, (c) oxygen cut normal quality series, (d) oxygen cut low quality series (e) plasma-arc cut normal quality series

Fig. 13 — A typical edge crack, machined specimen

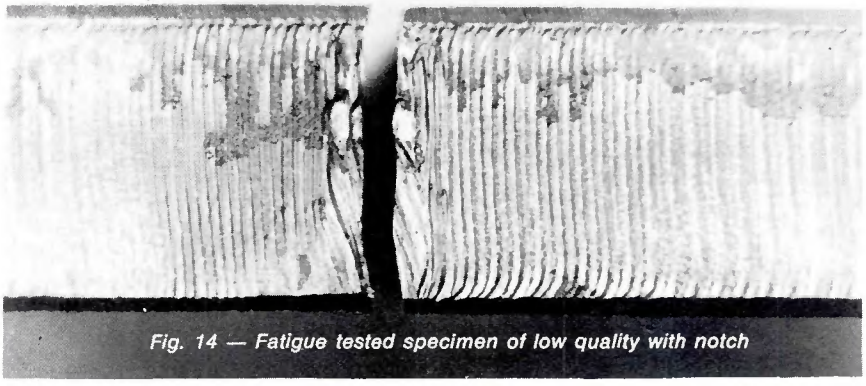

Fig. 14 — Fatigue tested specimen of low quality with notch

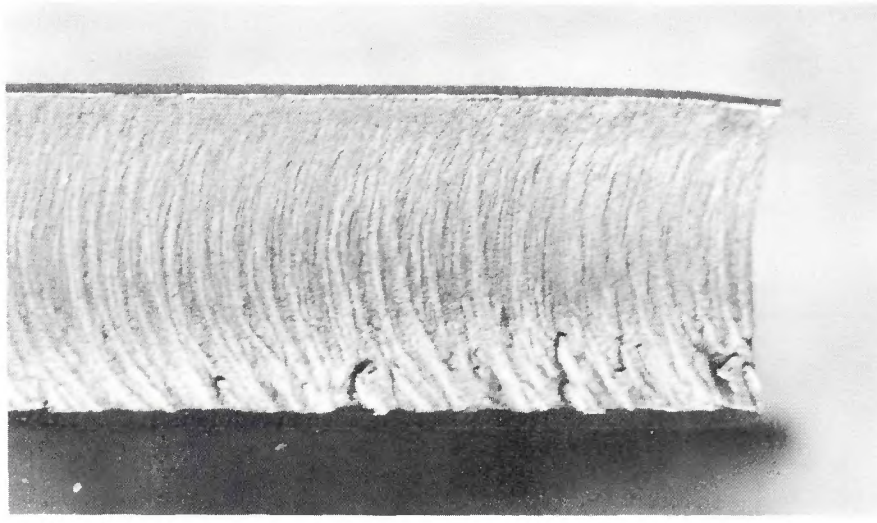

Fig. 15 — Rough plasma-arc cut surface caused by a defective nozzle, specimen E8x

Fig. 16 — Results of fatigue tests plotted as S vs log N curves showing the relation among the five quality levels tested

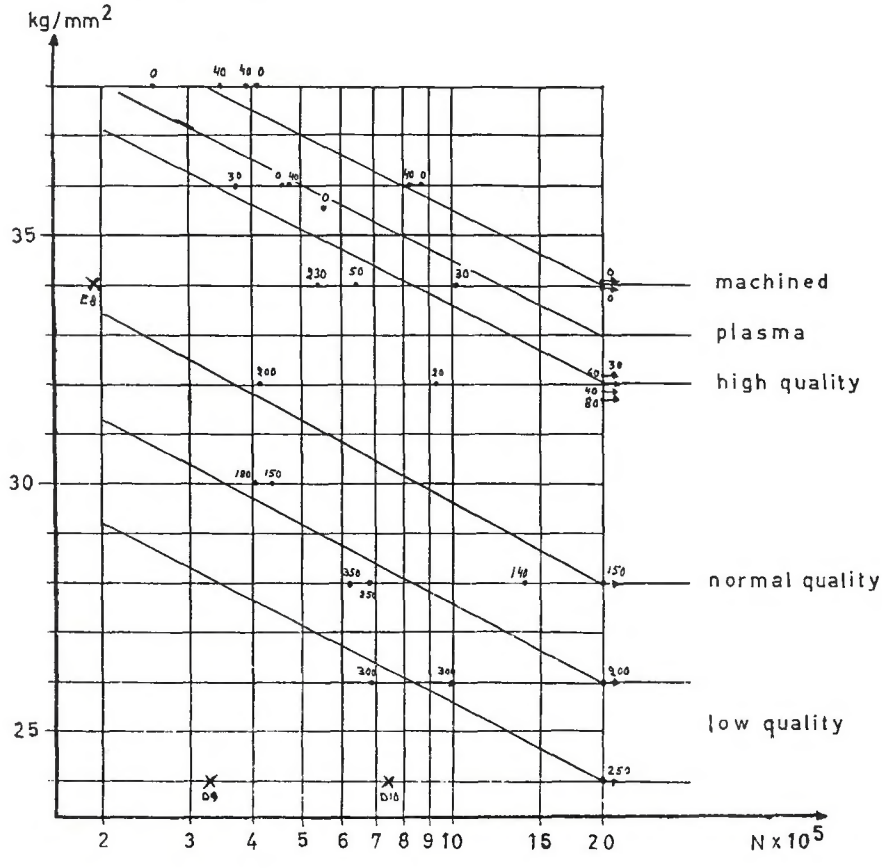

er the value of the profile ratio, the higher is the initiation effect from the cut surface. The profile ratio has been calculated for all the specimens and is listed in Table 2. If all specimens (including D 11 and D 12) that ran 2 × 10^6 cycles are plotted in a Profile Ratio — S diagram, Fig. 18, it is of interest to note that all points lie very close to a curved line and that the specimens D 11 and D 12 coincide well with the other points. As all the points form a curve which divides the diagram in two halves, A and B, it can be stated that, if a structure element has a profile ratio and σ_{max} within area A, the structure element should withstand fatigue. This of course is only true of the material used for this investigation. It is perhaps possible to make a general diagram if more fatigue tests could be made in steels with other analysis and mechanical properties.

Increased Fatigue Strength of Plasma-Cut Specimens

The plasma-arc cut specimens in this investigation have shown a high fatigue strength comparable to the results from the machined specimens, Fig. 12. As there is a difference in surface quality between these two series it is clear that not only the surface quality affects the fatigue strength but also the residual stresses in the cut surface. These were first studied by de Leiris and Ballet in 1952 (Refs. 9, 10) and recently by Ruge, Schimöller and Rao (Ref. 11).

Unfortunately no plasma-arc cut specimens have been investigated as yet in this respect, but, when studying the microstructure of oxygen cut specimens and their distribution of residual stresses, it is found that the material is under compressive stress where the microstructure consists of a martensite matrix. This is because the martensite crystal has a larger volume than the austenite it originated from. This implies that the plasma-arc specimens should have a better fatigue resistance because they have a deeper martensitic zone formed along the cut surface, which increases the compressive stress. Similar results have also been obtained by Sabelström (Ref. 12) who also found that, if the plasma-arc specimens were normalized, the fatigue resistance decreased, which confirms the above.

Factors Influencing Fatigue Strength

Geometry and Quality of Thermal Cut Surfaces

The geometry and quality of thermal cut surfaces are the most important factors concerning the fatigue strength of steel structures which this and other investigations have shown (Refs. 8, 12, 13, 14, 16).

Especially important is the condition of the upper edge, lower edge and cut surface. This is due to the stress concentration on the edges and at the bottom of the serrations on the cut surface. Figure 18 shows how increasing the profile ratio (initiation effect) reduces the fatigue strength. The residual stress distribution in the cut surfaces has also some influence on the initiation point of fracture which will be discussed later.

Initiation point of fracture. In this investigation the initiation point of fracture has varied depending on the surface quality. In the machined specimens the initiation point was mainly found on the edges, but two specimens fractured in the mill scale and one in the machined surface, Fig. 19. On the specimens of high and normal quality the edges are the main point of

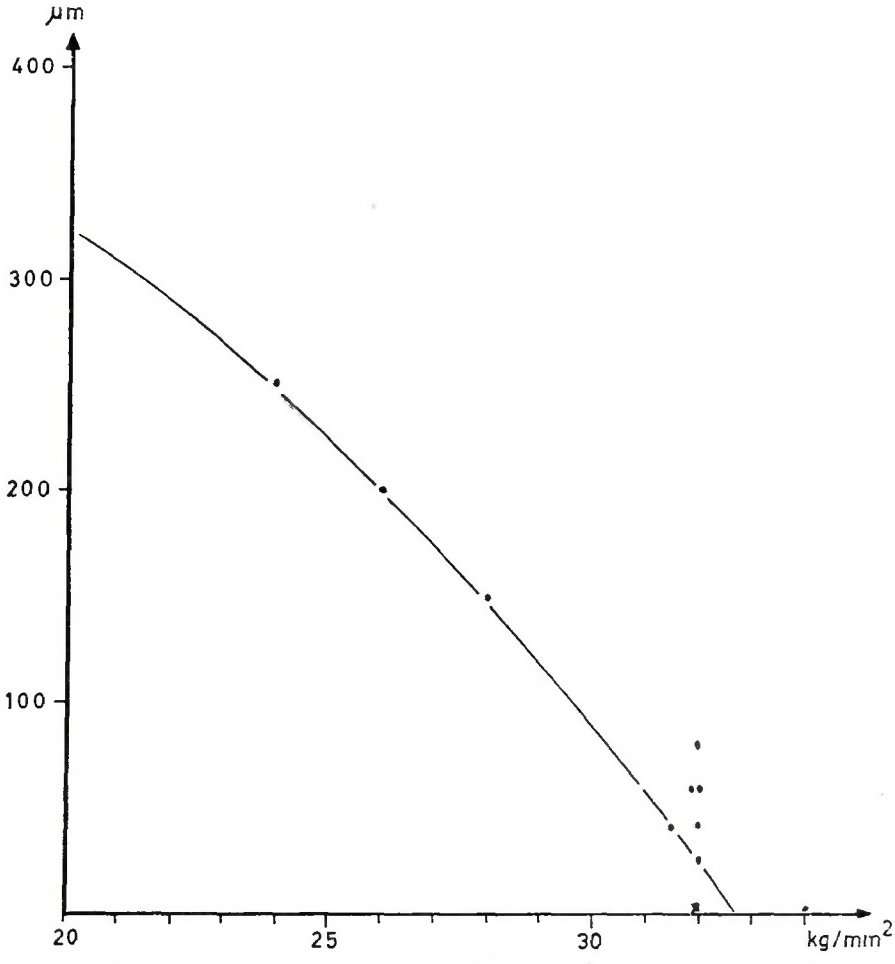

Fig. 17 — Plot of roughness (µm) vs S showing the relation between the roughness of the cut surface and the fatigue strength after $N = 2 \times 10^6$ cycles

initiation. When the cut surface had a low quality, the initiation point was often in the cut surface between two serrations.

When the oxygen cut edges are not chamfered, others have found (Refs. 13, 15) that fatigue cracks initiate only from the upper edge. The reason for this may be that the upper edge has a small zone of ferrite microstructure decarburized from the flame (Refs. 1, 2, 3). As ferrite has less fatigue strength than pearlite and pearlite/ferrite, it is logical that fatigue cracks are more frequent in the upper edge. If the edges are chamfered the fatigue strength increases 15% (Ref. 15). In this investigation all plasma-arc specimens fractured from the upper edge. So far there does not seem to be any proper explanation of this fact.

Notches. It is inevitable that notches will occur when a cut is lost or when a dirty cutting nozzle causes backfiring of the flame. As already shown in Fig. 16 and also found by other investigators (Refs. 7, 14, 16), these notches have a strong influence on the fatigue strength because they act as stress raisers. If a cut part has notches, it can be repair welded, when being used in a static structure. If the part will be put under dynamic stress it should not be repair welded. The reason for this will be discussed in a later paragraph. If the notch is small, it may be eliminated by grinding or milling, but if the notch is too deep to be ground or milled, the part must be rejected.

Residual Stresses

The residual stresses of oxygen cut surfaces have been studied by de Leiris and Ballet (Refs. 9, 10) and more recently by Ruge and Schimöller (Ref. 11). Their results show that the analysis and also to some extent the cutting parameters (cutting speed, size of flame and type of nozzle) control the residual stresses. When de Leiris and Ballet fatigue tested oxygen cut specimens of a nickel-chromium steel alloy of the 80 kg/mm² (114 ksi) class (unfortunately no analysis mentioned) the initiation point of fracture was found on the milled surface about 4-5 mm (0.16-0.20 in.) from the cut surface due to the positive stress concentration found at the same distance from the cut surface.

Measurements made by Ruge and Schimöller in St-E-36 steel (Ref. 17) show that the surface has a compressive stress (caused by the martensite) and a maximum strain about 1 mm (0.04 in.) behind the cut surface. If the fracture initiation is caused by this strain, the edge will be regarded as the initiation point since it is chamfered 1-2 mm.

Analysis and Strength of Steel

Results from Erker (Ref. 18) and de Leiris (Refs. 9, 10) indicate that the fatigue strength as a percentage of σ_s decreases with increasing amount of alloy elements and yield stress. When comparing the different investigations in the reference list, an average value of the fatigue strength of oxygen cut specimens with normal surface quality is 60-80% of the yield stress. The steels are of C-Mn type with C < 0.20%, which have a yield stress between 30 and 40 kg/mm² (42.3 and 56.5 ksi).

In low alloyed steels, which Erker and de Leiris used, the fatigue strength was 40-50% of the respective yield stresses.

Thickness

With increasing thickness of a steel plate, a higher degree of tri-axial tension is obtained which decreases the fatigue strength. Investigations (Refs. 13, 19) with oxygen cut specimens of different thicknesses have also proved this, but unfortunately they have not calculated the relation between the increasing thickness and the decreasing strength. In one investigation (Ref. 13), it was found that the initiation sensitivity of steel St 52 increases with thickness when compared with other normal structural steel types, such as St 37.

Heat Treatment

Normalizing and stress-relief heat treatment reduce the carbon concentration on the oxygen cut surface and decreases the hardness and the residual stress. Different investigations (Refs. 12, 16, 18) have shown that the heat treatment reduces the fatigue strength. The normalizing may decrease the yield stress and therefore reduce the fatigue strength but the reduction of the compressive stress is probably more important. Also plasma-arc cut specimens, which have no carburized edge, have a lower fatigue resistance after normalizing, which indicates the importance of compressive residual stress adjacent to the cut surface.

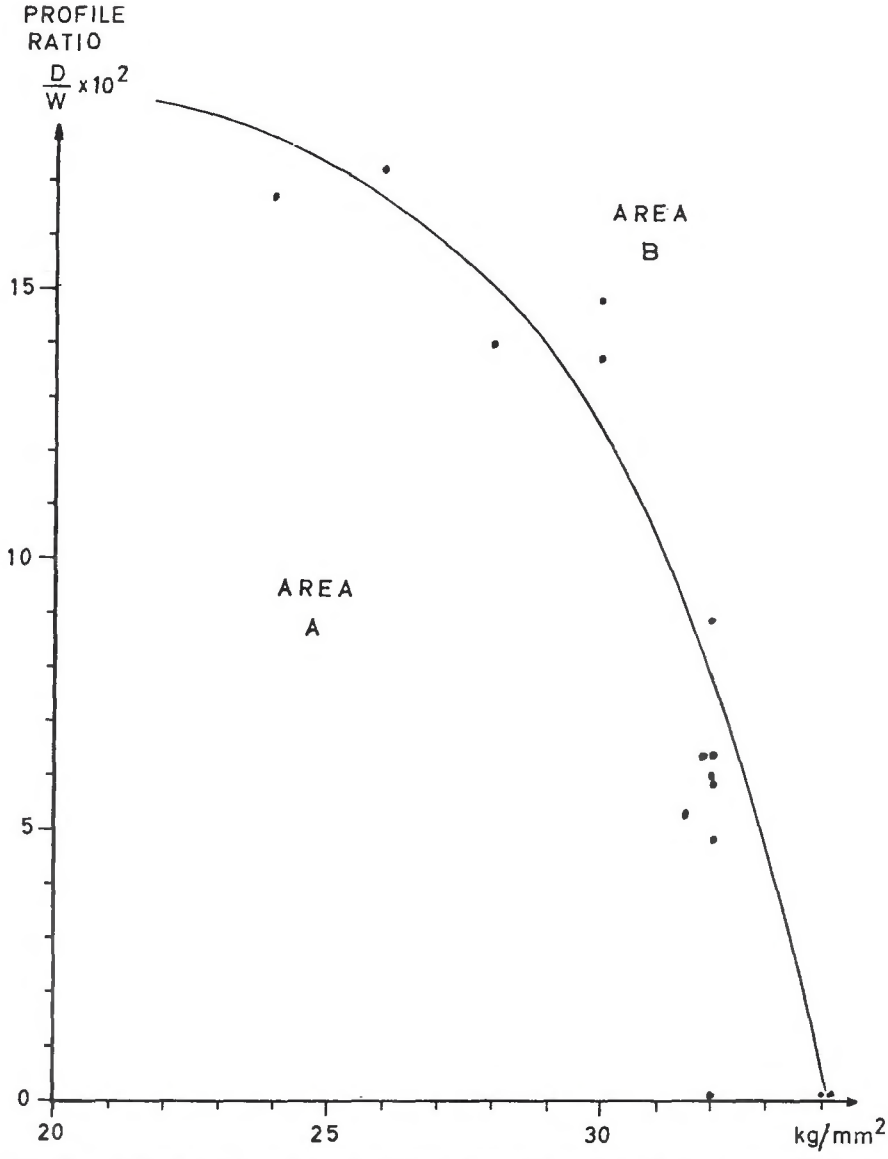

Fig. 18 — Plot of profile ratio vs S, showing how fatigue strength increases with lower profile ratio values

Fig. 19 — Initiation of fracture in the mill scale of a machined specimen

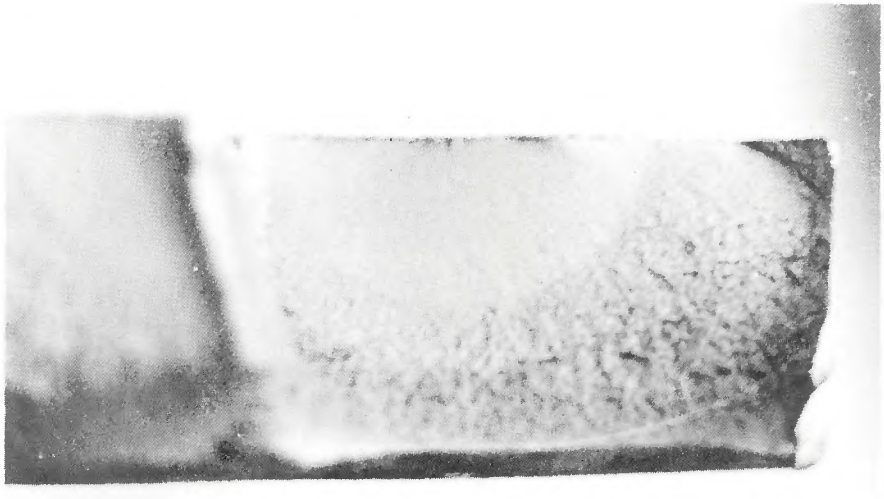

Repair Welding of Oxygen Cut Surfaces

Matting, Wolf and Steffens (Ref. 7) have investigated this problem and say that the test results of the repair welded specimens scattered more than only oxygen cut specimens and that properly repaired specimens with a ground weld bead, in general, had the same fatigue strength as oxygen cut specimens. After studying their diagrams, this author would not make the same conclusion. The results show very large scatter and very few specimens have run 2×10^6 cycles. Others (Ref. 12) found on the contrary that weld-repaired specimens had a very poor fatigue resistance. These results are natural when considering the complex residual stress obtained when repair welding the oxygen cut surface. It should be noted that the present investigation does not encompass the condition where repair-welded cut surfaces are subsequently welded to other components of a structure.

Other Treatments

Sand Blasting. Sabelström (Ref. 12) and Erker (Ref. 18) sand blasted cut surfaces until the serrations disappeared. This operation removes the thin brittle carburized layer and is thought to induce extra compressive stress that increases the static and fatigue strength. The fatigue strength after this treatment is slightly better than that of as-machined surfaces.

Hot Galvanizing. If an oxygen cut surface is hot galvanized, the fatigue strength is drastically reduced and is about 30% of the yield stress. The fractures start from the cut surface probably due to zinc penetration in grain boundaries, forming microcracks (Ref. 12). These microcracks may form in the thin brittle surface layer and during fatigue testing act as notches.

Comparison of Rolled and Sheared Edges

It is also of interest to know how the fatigue strength of oxygen cut surfaces compare with rolled and sheared edges. It is of course very difficult to have rolled or sheared edges prepared on normal test pieces with radii. Shiskin and Kaugan (Ref. 19) welded T-bars which were tested in fatigue bending with the plate edge under examination in the maximum tensile stress zone. They found that specimens with rolled edges of high quality had better fatigue strength than the oxygen cut specimens. However, if the rolled edge was defective, the fatigue strength fell to a much lower level than obtained with planing or shearing. In 16 mm (⅝ in.) thick plates they found that the fatigue strength of oxygen cut specimens was

77% of the rolled specimens and that of the sheared specimens was 57% of the rolled specimens.

Friis (Ref. 20) compared the fatigue strength of rolled and oxygen cut edges by using test specimens without a radius. One series of specimens had both sides oxygen cut with normal quality and another series had one side rolled and one side oxygen cut. Of thirteen test pieces only two fractures started from the rolled edge, four from the mill scale and seven from the oxygen cut surface. The reason for this distribution may be that, when the specimens were cut on one side only, they were slightly curved, but the results show, however, no specific difference in fatigue strength between the oxygen cut and the rolled specimens. In both series the fatigue strengths were 77% of the yield stress.

References

1. Goldberg, F., "The Source of Increased Carbon Content in Gas Cut Steel Surfaces," *Welding in the World,* 1971, vol 9, no 7/8; also *Indian Welding Journal,* 1972, vol 4, no 1; also "Origine de l'accroissement de la teneur en carbone à la surface des coupes dans l'oxycoupage des aciers," *Soudage et Techniques Connexes,* Paris, 1971, vol 26, no 1/2.

2. Goldberg, F., "Kolkoncentrationen i gasskurna snitt," *Svetsen,* 1971, Nr 6.

3. Goldberg, F., Fredriksson, L. and Norén-Brandel, T. M., "Gas Cutting of Structural Steels at Low Temperatures" International Institute of Welding, Document I-482, 1972.

4. Antonov, A., Spektor, O. and Trofimov, A. A., "Evaluation of the Quality of the Cut Surface in Oxygen Cutting," *Svar. Proiz,* 1969, No 12, p. 11-13.

5. Hofman, W. und Krahl, A., "Werkstoffveränderungen in der varmebeeinflussten Zone Autogener Brennschnitte," *Schweissen & Schneiden,* 1963, Heft 4, p. 153.

6. Ito, T., "Characteristics of Plasma Flame in Metal Cutting," Kameido Works, Hitachi Ltd, Febr. 1970.

7. Matting, A., Wolf, H. and Steffens, H-D., "Fatigue Strength of Flame Cut Steel Specimens Repaired by Welding," *Schweissen & Schneiden,* 1959, Heft 1, p. 8.

8. Boeckhaus, K. und Lenk, W., "Werkstoff und Brennschnitt Vorträge zur Grossen Schweisstechnischen Tagung" DVS, Düsseldorf, 1955.

9. de Leiris, H. and Ballet, M., "Contribution a l'étude de l'influence de l'oxycoupage des toles sur leur resistance á la fatigue," *Soudage et Techniques Connexes,* 1952, Nr 11/12, p. 271.

10. de Leiris, H., "Remarques sur les Can Oxycoupés," Association Technique Maritime et Aéronautique, Paris, Session 1955.

11. Rao, K., Ruge, J. and Schimöller, H., "Bestimmung der durch Brennschneiden von Stahlblechen verursachten Eigenspannugen," *Forschung im Ingenieurwesen,* 1970, Bd 36 Nr 6, p. 192.

12. Sabelström, S., Utmattningshallfastheten hos material med termiskt skurna kanter," Stalbyggnadsinstitutet, Stockholm, Nordiska Forskningsdagar, 1970, sessuib 1,6:1.

13. Schlebech, E., Müller, G.och Böiter, H. "Brennschneiden und Daüerfestigkeit von St 52-3," *Schweisstechnik* (Berlin), 1964, Heft 5, p. 302.

14. Robakowski, T. and Juffy, E. A., "Fatigue Strength of Gas Cut Steel St-52," International Institute of Welding, Doc I-1014-65.

15. Koeningsberger, F. and Garcia Martin, Z., "Fatigue Strength of Flame-Cut Specimens in Bright Mild Steel," *British Welding Journal,* 1955, Nr 1, p. 37.

16. Koeningsberger, F. and Green, H. W., "Fatigue Strength of Flame Cut Specimen in Black Mild Steel," *British Welding Journal,* 1955, Nr 7, p. 313.

17. Ruge, J. and Schimmöller, H., "Berechnung von Eigenspannugen in brenngeschnittenen Stahlblechen aus St E 36." Schweisstechnik, Soudure (Zürich), No. 7, 1972, p. 182.

18. Erker, A., "Festigkeitsversuche mit brenngeschnittenen Proben aus Cr-V-Stahl," *Schweissen und Schneiden,* 1953, Nr 5, p. 183.

19. Shishkin, V. and Kaugan, V. A., "Influence on the Fatigue Strength of Structural Members of the Edge Preparation Technique," *Svar. Proiz,* 1970, p. 25.

20. Friis, L-E., "Utmattningshållfastheter hos plåt och universaljärn med gasskurna kanter kvalitet NVA 36," Laboratorierapport LM 80/69 Gränges Stål, Oxelösund, Sweden.

Acknowledgements

I am indebted to Professor T. M. Norén-Brandel, Dept. of Welding Technology for arranging excellent facilities at my disposal. I also wish to thank L-E. Friis, Gränges Stål, Oxelösund, and J-E. Holmström, Dept. of Welding Technology, for valuable help and discussion and also Gränges Stål, Oxelösund, for supplying the steel for this investigation.